ELSEVIER

Contents lists available at ScienceDirect

Bioresource Technology

journal homepage: www.elsevier.com/locate/biortech





Insights into the roles of biochar pores toward alleviating antibiotic resistance genes accumulation in biofiltration systems

Lecheng Wei a,d , Jingjing Zheng a,d , Yutong Han a,d , Xiangyang Xu a,b,c , Mengyan Li e , Liang Zhu a,b,c,d,*

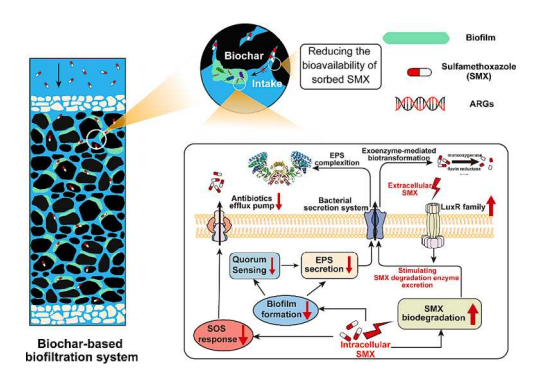
- a Institute of Environment Pollution Control and Treatment, College of Environmental and Resource Science, Zhejiang University, Hangzhou 310058, China
- ^b Zhejiang Province Key Laboratory for Water Pollution Control and Environmental Safety, Hangzhou 310058, China
- ^c Zhejiang Provincial Engineering Laboratory of Water Pollution Control, Hangzhou 310058, China
- ^d Innovation Center of Yangtze River Delta, Zhejiang University, China
- e Department of Chemistry and Environmental Science, New Jersey Institute of Technology, Newark, NJ, 07102, USA

HIGHLIGHTS

Biochar pores effectively reduced ARG accumulation in biofiltration systems.

- Metagenomic and metaproteomic analyses elucidated microbial metabolism response.
- Biochar pores affected the microbial defense strategy against antibiotic stress.

GRAPHICAL ABSTRACT



ARTICLE INFO

Keywords:
Biochar
Pore
Biofiltration system
ARGs
Microbial metabolism

ABSTRACT

Biofiltration systems would harbor and spread various antibiotic resistance genes (ARGs) when treating antibiotic micro-pollution, constituting a potential ecological risk. This study aimed to investigate the effects of biochar pores on ARG emergence and related microbial response mechanisms in bench-scale biofiltration systems. Results showed that biochar pores effectively reduced the absolute copies of the corresponding ARGs sul1 and sul2 by 54.1% by lowering the sorbed-SMX's bioavailability compared to non-porous anthracite. An investigation of antimicrobial resistomes revealed a considerable decrease in the abundance and diversity of ARGs and mobile gene elements. Metagenomic and metaproteomic analysis demonstrated that biochar pores induced the changeover of microbial defense strategy against SMX from blocking SMX uptake by EPS absorbing to SMX biotransformation. Microbial SOS response, antibiotic efflux pump, EPS secretion, and biofilm formation were decreased. Functions related to SMX biotransformation, such as sadABC-mediated transformation, xeno-biotics degradation, and metabolism, were significantly promoted.

^{*} Corresponding author at: Department of Environmental Engineering, Zhejiang University, No. 866 Yuhangtang Road, Hangzhou 310058, PR China. *E-mail address*: felix79cn@zju.edu.cn (L. Zhu).

1. Introduction

Antibiotics are broadly employed as efficacious therapeutic and prophylactic agents and animal growth promoters in human healthcare, livestock husbandry, and aquaculture (Ajibade et al., 2023). The extensive discharge of antibiotic residues into the aquatic environment has caused an enormous burden of antibiotic selection pressure on indigenous microorganisms. This stimulated the accelerated emergence and dissemination of antibiotic resistance genes (ARGs), seriously threatening human and ecological health (Tang et al., 2023). To lessen the adverse environmental effects of human-origin antibiotics, biofiltration systems (BFs) have been recommended as an efficient, economical, and sustainable technology to control both point and nonpoint source pollution containing antibiotics (Deng et al., 2021). However, microbial biofilms in biofiltration systems would evolve into ideal reservoirs for developing and spreading ARGs under the continuous selection pressure of retained antibiotics (Guo et al., 2018; Xu et al., 2020). Therefore, reducing the potential of ARG accumulation and dissemination is crucial to lessen the environmental risks and promote the broad application of biofiltration systems in tackling antibiotic

As the primary function carrier for intercepting pollutants and habituating microbial biofilms, the filter media is a critical component in biofiltration systems. Its properties, including surface characteristics, specific surface area, and pore distribution, affect intercepted pollutants' adsorption behavior and bioavailability. The filter media also significantly impacted the microbial community composition and core microbiomes of biofilms colonizing in biofilters (Liang et al., 2023). Variation in antibiotic resistomes of biofilms during the biofiltration process is generally associated with the microbial community (Xu et al., 2020). Zheng et al. (2018) found that the persistent ARGs were primarily linked with Firmicutes in activated carbon biofilms. Xu et al. (2020) reported GAC media were more closely associated with intI1 than other sand or anthracite-sand biofiltration systems. They attributed the highest RP1 plasmid transfer frequency on GAC media to the increased surface area and unique pore structure of GAC, which induced bacterial collision, attachment, and more frequent conjugation. These observations suggested filter media play a crucial part in modifying ARG occurrence and resistomes in biofiltration systems. However, limited studies have explored the relationships between filter media properties and ARG occurrence. How to alleviate ARG accumulation and dissemination via selecting applicable media or selectively modifying its properties requires more exploration.

Biochar is an efficient and environment-friendly carbon material widely applied for pollution remediation of antibiotics and ARGs (Su et al., 2015; Zhu et al., 2017). Biochar shows a potential to reduce the absolute abundance of ARGs and mitigate ARG pollution in the soil (Zhu et al., 2017), mainly via lowering contaminant availability and regulating community structure, as well as resistomes. Then, biochar may serve as an ideal filter media for the prevention of antibiotic pollution. However, the high biocompatibility of biochar would promote microbial attachment and biofilm formation, potentially accelerating the horizontal gene transfer (HGT) and the spread of ARGs (Xu et al., 2020). He reported that GAC media showed greater integron-mediated ARG exchange in GAC biofilters than in other sand or anthracite-sand biofilters. These studies imply an uncertainty of biochar application for ARG alleviation in biofiltration systems. The feasibility of biochar-based biofiltration systems to control antibiotics and ARG pollution remains to be evaluated. And pore structures, the critical property of biochar, were found to decrease the bioavailability of sorbed antibiotics and lower the ARG activation of adjoining microbes (Wang et al., 2020). The pore size distribution of biochar also plays a vital part in microbes' community composition and metabolic activity (Lu et al., 2022). Very limited studies have investigated biochar pores' crucial role in remediating ARG accumulation in biofiltration systems. Nevertheless, there is still a lack of understanding of how biochar pores affect the ARG

emergence and dissemination in biofiltration systems.

In this study, two biofiltration systems comprising two types of common carbonaceous materials, non-porous anthracite, and porous biochars, were set up at bench-scale to purify the wastewater containing antibiotics. It aims to investigate (i) the effects of biochar pores on ARG accumulation in filter biofilms and (ii) the intracellular pathways through which biochar pores affect ARG occurrence and dissemination. Furthermore, metagenomic and proteomic analysis was conducted to reveal the possible mechanisms of the mitigation effects of biochar pores on ARG emergence in biofiltration systems. Overall, the results of this study could enhance the understanding of the relationships between filter media properties and ARG occurrence in biofiltration systems.

2. Materials and methods

2.1. Biofiltration system setup and operation

Non-porous anthracite (AnC) and porous biochars (BioC) representing two biofiltration systems, named AnF and BioF, were set up in parallel at bench scale. Each biofiltration system type was operated in duplicate (see Supplementary materials). The biofiltration systems consisted of six PVC columns (8 cm inner diameter × 60 cm length), filled with 10 cm of support gravel and 40 cm of filter media (AnC: effective size (ES) 0.80 mm, uniformity coefficient (UC) 1.28; BioC: ES 0.54, UC 1.83; porosity, 0.32). The anthracite and biochar pyrolyzed from coconut shells were all purchased from the Lvlin activated-carbon ltd in Pingdingshan City, China. The characteristics of the filter media were analyzed in terms of surface functional groups and pore distributions (see Supplementary materials). The biofiltration systems were operated under a hydraulic loading rate of 0.25 cm/h, resulting in a hydraulic retention time of 10 h. All columns were operated for 254 days at room temperature (25°C) without light.

The feedwater for all biofiltration systems was simulated synthetic wastewater, of which the water quality referred to the common nonpoint source wastewater in China (Liu et al., 2018). The synthetic wastewater was prepared by adding sodium acetate, NH₄Cl, KNO₃, and KH₂PO₄, where the concentration was approximately 40 mg·L $^{-1}$ TOC, 8 mg·L $^{-1}$ NH $^{+}_{4}$ -N, 8 mg·L $^{-1}$ NO $^{-}_{3}$ -N, and 1 mg·L $^{-1}$ total phosphorus (TP). In this study, sulfamethoxazole (SMX), the first widely used sulphonamide antibiotic, was selected as the representative antibiotic. SMX in the synthetic wastewater was set to be \sim 2 μ M (equivalent to 500 μ g-SMX·L $^{-1}$), referring to the reports of real wastewater in China (Oberoi et al., 2019).

2.2. Analytical methods

The concentration of total organic carbon (TOC) of the influent and effluent was measured by a TOC analyzer (TOC-L, Shimadzu). The concentration of SMX in the filtrate was analyzed by UPLC-MS (Acquity SQD2, Waters) using a 2.1×50 mm BEH C18 column (1.7 µm, Waters) and detailed quantitative methods were referred to Oberoi et al., 2019. The mobile phases were A: deionized water + 0.1 % formic acid and B: acetonitrile + 0.1 % formic acid. Gradient elution was used for optimum separation, and it was as follows: 5 % B p (0–1 min), 5 % $\rightarrow50$ % B (1–4 min), 50 % $\rightarrow50$ % B (4–4.5 min), 5 % B (4.5–5 min). SQD2 mass spectrometry detector with ESI source was operated in positive ionization mode. The mass spectrometry parameters were as follows: SIR mode, capillary voltage: 2.70 kV, cone voltage 40 V, source temperature 200° C, desolvation gas flow of 500 L/h nitrogen gas. The limit of quantification (LOQ) was 1 ug/L, defined as ten times the ratio of signal to noise.

Extraction and quantification of EPS were as follows. In brief, three media samples (2–4 g) were collected from each biofilter column's bottom, middle, and upper layers on days 177, 218, and 255 and were mixed as a sample. Then, they were added to a sterile tube with 10 mL of extraction buffer (10 mM Tris, 10 mM EDTA, 2.5 % NaCl, pH 8). After vortexing for 1 min, they were incubated for 4 h at 35 °C while shaken at

200 rpm. Polysaccharides (PS) and proteins (PN) in the extractant were measured by a modified phenol–sulfuric acid colorimetric method and the Pierce bicinchoninic acid (BCA).

The EEM fluorescence spectra of EPS extraction liquids were obtained using a fluorescence spectrophotometer (Hitachi F-4600, Japan) to identify the organic compositions. The biofilm staining was employed to visualize the distribution of live/dead cells using the live/dead baclight bacterial viability kit (L13152, Thermo Fisher Scientific Inc.) following the manufacturer's instructions. $\sim 0.5~g$ filter grains were mixed with 100 μL mixture of SYTO 9 (2.5 $\mu mol/L)$ and propidium iodide (2.5 $\mu mol/L)$ and incubated at room temperature in the dark for 20 min. Biofilms were imaged via confocal laser scanning microscopy (CLSM, FV3000-Olympus, Japan) with 485 nm (SYTO 9) and 561 nm (PI). CLSM images were processed by FV31S-SW (version 2.1).

For biodegradation tests, 20 mL bacterial suspensions detached from the filter media (~ 3 g) on 252 days were mixed with 100 mL of sterilized influent in a 250 mL Erlenmeyer flask. SMX concentration was recorded at 6, 12, 18, 24, 36, 48 h. The SMX removal normalized to 16S rRNA copies served as the indicator of the SMX degradation capacity of biofilm. Adsorption experiments were conducted in duplicate at $25\pm0.5\,^{\circ}\text{C}$ for 24 h and an adsorbate-water ratio of 5 g/L. Initial concentrations of SMX were 1, 5, 10, 20, 30, 40, 5and 0 mg/L. Adsorption equilibrium data were fitted with the Freundlich isotherm model: $Q_e = K_F C_e^{1/n}$, where Q_e is the amount of SMX adsorbed on adsorbent at equilibrium (mg/g), C_e is the equilibrium concentration of SMX in solution (mg/L), and K_F and n are the Freundlich constant and empirical parameter, respectively.

For the extraction of absorbed SMX, $\sim\!\!1$ g filter grains from the biofilter columns on 240 days were mixed with 10 mL of acetonitrile in a 15 mL extraction vial. The mixture was then sonicated with a 45 kHz ultrasound at 30 °C for 2 h. The supernatant was filtered through a 0.22 μm filter and analyzed to determine SMX concentration.

2.3. Sample collection, DNA extraction, and qPCR

Triplicate filter media grains (1–3 g) were collected from each bio-filtration system's bottom, middle, and upper layers on days 177, 218, and 255 and mixed as individual samples. Then, filter media samples were transferred into sterile Erlenmeyer flasks with 30 mL desorption solution, followed by low energy sonication (100 W, 10 min) and sonication probe (27 W, 300 sec) dipping to detach bacterial biofilms. The desorption solution consisted of 10 mM sodium pyrophosphate and 5 % Tween 80 (Vignola et al., 2018). The bacterial suspension was concentrated by ultracentrifugation (Allegra 64R, 10000 rpm, 10 min), and cell pellets were collected and stored at -80° C until DNA extraction. Genomic DNA was extracted using the DNeasy® PowerSoil® Kit (QIA-GEN, Germany).

Quantification of sulfonamide resistance genes and microbial biomass was conducted by real-time qPCR, which quantified the absolute copy numbers of the $sul1,\,sul2,\,$ and 16S rRNA genes. Primers for $sul1,\,sul2,\,$ and 16S rRNA were referred to by Zhu et al. (2017). The qPCR reactions were performed with a real-time PCR system (LightCycler480 II, Rotkreuz, Switzerland) in a 25 μL reaction mixture (10 \times PCR buffer (Sangon Biotech), 0.2 μM of each primer, and 2 μL of template). The thermal cycling conditions consisted of an initial 3 min pre-heating at 95 °C, followed by 35 cycles of denaturation for 30 s at 95 °C, annealing for 30 s at 57 °C, and extension for 30 s at 72 °C. And the final step in the run was a DNA extension at 72 °C for 8 min.

2.4. Metagenome sequencing and analysis

Genomic DNA sequencing was performed using the Illumina Hiseq platform at the Allwegene Co Ltd in Nanjing, China. In total, 0.67 billion raw reads were acquired from all samples and assembled via MEGAHIT (v1.2.9) based on the De-Brujin graph mechanism. Assembled contigs

longer than 800 bps were reserved for the subsequent gene prediction. The ORF prediction was used by the Prodigal (v2.6.3) and CD-HIT software (v4.8.1, set as -c 0.95 -aS 0.85 -M 0 -d 0) to eliminate the redundancy. Bowtie2 software (v2.5.1) was used to align the assembled reads to the non-redundant gene catalogs to estimate gene abundance. DIAMOND software (v2.1.8, set as blastp; e-value $\leq 1e^{-5}$) was used for the taxonomic and functional annotations by assessing the gene catalogues using NR (2023, blastp, e-value $\leq 1e^{-5}$), KEGG (v108.1), eggnog (v5.0), and CAZy databases (2023). The specific parameters have been added, and other software tools were operated in their default parameters.

For ARG annotation, non-redundant gene catalogues were applied to search against the Comprehensive Antibiotic Resistance Database (CARD, 2023) database using the RGI software (v6.0.0). For mobile genetic element (MGE) annotation and analysis, construction, and screening of a local database were referred to Guo et al. (2017) with an E-value threshold of 10-5. The proportion of each ORF was normalized by salmon (v1.7.0) and defined as "abundance" (using the unit of "TPM," Transcripts per kilobase of exon model Per Million mapped reads).

2.5. Protein preparation and proteomic analysis

The protein extraction and proteomic analysis was referred to Lu et al. (2020). DDA and DIA raw data were acquired using Orbitrap Fusion Lumos and Easy nanoLC 1000 (Thermo Scientific). All DDA raw data were uploaded to the Sequest HT (v1.4) node integrated into the Proteome Discoverer (PD) software (v2.1, Thermo Fisher Scientific) and searched against the Mouse Uniprot fasta database (83625 entries, downloaded on Mar 18, 2019) coupled with the Biognosys iRT peptide sequences. Function annotation of the identified proteins was performed against the NCBI NR, KEGG, CAZy, and GO databases.

2.6. Statistical analysis

All experiments were conducted in triplicate for the stability and reliability of the data. Results were shown as mean \pm standard deviation. One way analysis of variance (ANOVA) and Tukey's Honest Significant Difference (HSD) were applied to evaluate significant differences between experimental groups, with p<0.05 and p<0.01 chosen as the significant values. R(4.0.3) with ggplot2 and pheatmap packages were applied to draw heatmaps and bubble chart, of which the data were acquired from metagenomic analysis. The results were visualized by Adobe Illustrator (2019). The correlation analysis was performed with Hmisc packages in R.

3. Results and discussion

3.1. Performance and SMX removal in BFs

During 254 days of operation, manure biofilms colonized the filter media (see Supplementary materials). AnC and BioC filter eventually turned into the biological filtration systems and removed over 90 % TOC (Fig. 1a). The average TOC concentration in the effluents of AnBF and BioCF were 2.10 ± 0.51 and 3.25 ± 0.85 mg/L, respectively. Owing to the higher affinity of BioC on SMX than AnC (Fig. 1c, d), BioCF also efficiently removed over 95 % SMX and the average effluent SMX concentrations were 4.30 $\hat{A}\pm1.65~\mu g/L$. However, the average SMX removal rate of AnBF was just 31.4 %.

The analysis of biofilm morphology showed that the AnC surface was colonized by the compact and dense biofilms, in which more dead cells were present than in BioCF (see Supplementary materials). The EPS contents of biofilms in AnBF increased significantly from 0.25 $\hat{A}\pm0.011$ mg/g to 0.73 $\hat{A}\pm0.023$ mg/g from day 177 to day 255. It was significantly three times higher than in BioCF (p < 0.05). It is worth

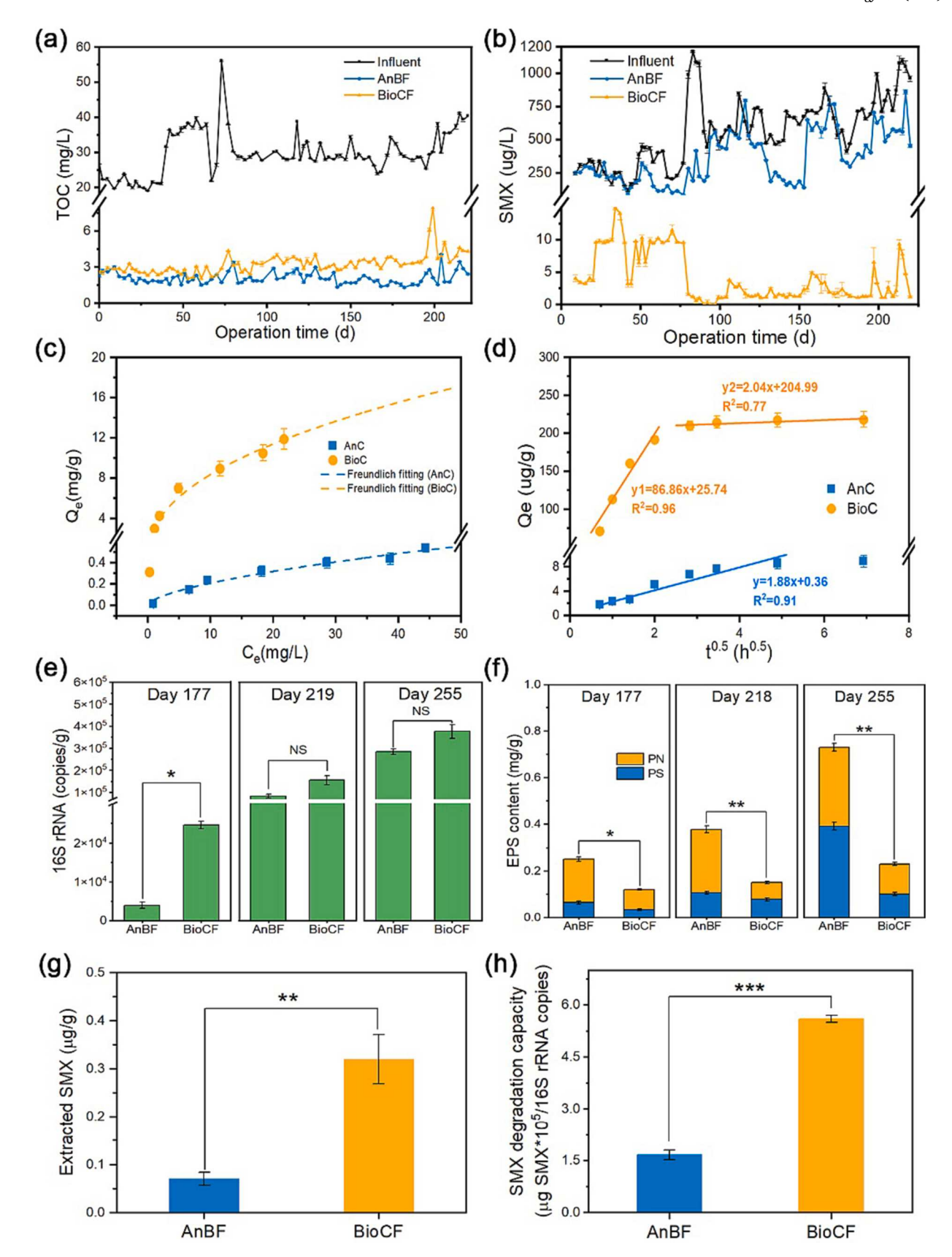


Fig. 1. The TOC (a) and SMX (b) removal performance of BFs. Adsorption isotherm of SMX on AnC and BioC by Freundlich isotherm fitting (c). Adsorption kinetics of SMX on AnC and BioC fitted by Weber and Morris (W&M) model (d). The amount of extracted SMX from filter media after 250-days' operation (g). The SMX degradation capacity of biofilms detached from filter media on day 254 (f). Note: *, p < 0.05; **, p < 0.01; NS, no significance.

mentioning that the biomass contents, represented by 16S rRNA copies in AnBF and BioCF, are similar (p > 0.05) (Fig. 1e). Proteins, as the main components of EPS, are thought to shelter microbes from antimicrobial stress via various functional groups (e.g., carboxyl, amine and hydroxyl groups) (Zhang et al., 2018). The higher EPS contents of AnBF are thought to be related to higher SMX stress. The sorbed-SMX extraction results further showed that 0.07 $\hat{A}\pm0.01$ and 0.32 $\hat{A}\pm0.005\,\mu\text{g/g}\,\text{SMX}$ was recovered from AnC and BioC, respectively. In summary, it was inferred that much less interpreted SMX by AnBF still exerted more considerable selective pressure on the microbial biofilms than in BioCF.

3.2. Occurrence of ARGs against SMX stress

3.2.1. Sul ARGs

Long-term stress from sorbed SMX would induce the accumulation of microbial resistance against SMX in biofilms. As shown in Fig. 2a, the biofilm in AnBF carried the most copies of sul genes (including sul1 and sul2) at 81439.8 Å \pm 1528.0 copies/g after 255 days of operation. Compared to AnBF, the absolute copies of sul genes in BioCF significantly decreased by 54.1 % (p<0.05). The relative abundance of sul genes was calculated by normalizing the sul-gene copies to the 16S rRNA copies. Fig. 2b illustrated the relative abundance of sul ARGs in BioCF, 0.07 Å \pm 0.004, decreased by 75.9 % compared with that in AnBF, 0.29 \pm 0.02. The higher abundance or relative abundance of sul ARGs in AnBF further verified that microbes in AnBF suffered from much more SMX exposure and selection stress.

The difference in SMX selection stress in the two BFs was closely linked with the bioavailability of retained SMX. The SMX removal from wastewater by BFs mainly relied on the adsorption of filter media, which can be further classified as surface adsorption and pore restriction. Microbes colonizing filter media prefer to utilize organic matter absorbed

by the media (Lu et al., 2020). For the non-porous AnC, the absorbed SMX on the surface may be detached under the effects of soluble microbial products and displayed high bioavailability. For the porous BioC, the area ratio of external surface and pores with a diameter below 200 nm, which can't be reached by microbes, was just 0.58 (see Supplementary materials). Combined with the fast diffusion kinetics of BioC (Fig. 1d), these meant most adsorbed SMX was located in the micropores and mesopores of BioC. The pore-limited continuity restricted the desorption of SMX to the media surface. The steric hindrance effects of pores significantly reduced the bioavailability of sorbed SMX (Wang et al., 2020). Much higher SMX contents extracted from BioC than AnC also strengthened the result (Fig. 1g). Owing to the similar surface functional groups between BioC and AnC, the effects of surface property of filter media on the bioavailability of sorbed SMX weren't taken into consideration. In summary, biochar pores effectively lowered the bioavailability of sorbed SMX by pore filling and mitigated its exposure and selection stress.

3.2.2. Resistomes and mobile gene elements (MGEs)

According to the analysis of metagenomic sequencing, 12 types of ARGs, including 67 subtypes, were detected in two BFs (Fig. 3a, c). It was evident that the abundance of most kinds of ARGs in BioCF was lower than that in AnBF. The abundance of the total ARGs in BioCF significantly decreased by 60.3 % (p < 0.01). Considering collateral enrichment of non-corresponding ARGs by individual-specific antibiotics, many other non-corresponding resistance genes were also depleted. Among these ARGs, genes that resisted to sulfonamide, aminoglycoside, fluoroquinolone, and tetracycline were the main types in all samples (see Supplementary materials).

In addition to resistomes, Fig. 3b illustrated the variations in MGEs, i. e., plasmids, insertion sequences (IS), and integrons, to further evaluate

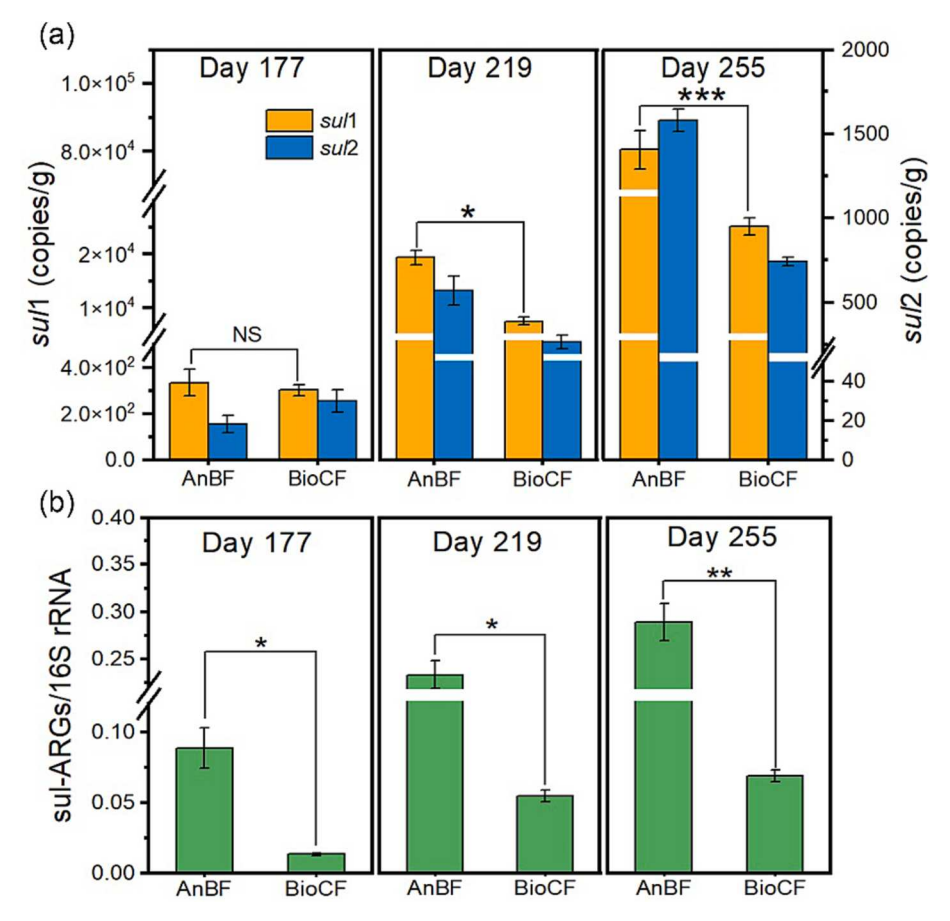


Fig. 2. The sul-ARGs copies (a) and the ratio of sul ARGs to 16S rRNA of the biofilm attached to biofilter media (b).

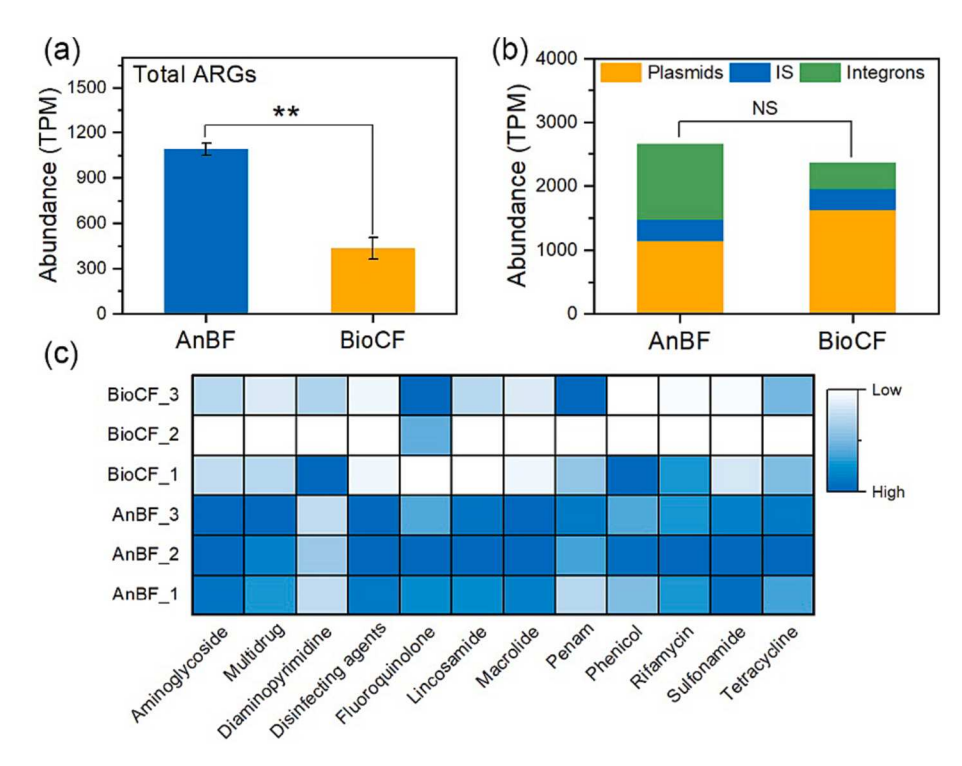


Fig. 3. The relative abundance of total ARGs (a) and MGEs (b) in the BFs. The abundance of each type of ARGs (heatmap) in each biofilm sample from the BFs (c).

ARGs' horizontal gene transfer potential. The abundance of total MGEs decreased by just 11.2 % despite much lower SMX stress in BioCF (p > 0.05). A total of 1406 types of plasmids, 18 types of integrons, and 28 types of IS were detected in all samples (see Supplementary materials). The abundance of integrons in AnBF was significantly 2 times higher than that in BioCF (p < 0.05) while no noticeable difference existed in terms of plasmids and ISs. Among them, intI1 was the most common and important, accounting for about 20 % of all samples. IntI1 was reported to be associated significantly with ARGs and promoted the emergence of HGT (Zhao et al., 2021).

In summary, biofilms in BioCF suffered from far lower SMX stress under the sheltering effects of biochar pores and accumulated much less ARGs, which showed lower HGT potential.

3.3. Alternation of microbial community

Variations in antibiotic resistomes during biofiltration processes are generally associated with the microbial community composition (Xu et al., 2020). During the 254-day run, BioCF and AnBF displayed obviously different bacterial communities. Proteobacteria became the most dominant phylum (relative abundance exceeding 60 %) in two BFs, followed by Chloroflexi (9 %) and Bacteroidetes (3 %) (see Supplementary materials). The enrichment of Proteobacteria might be owing to the phospholipid bilayer of Proteobacteria, which can readily interact with SMX (Chen et al., 2023). This made Proteobacteria more sensitive to SMX stress and more likely to elicit response behavior. At the genus level, the relative abundance of Rhodoplanes, Bradyrhizobium, and Desulfomonile in BioCF significantly increased by over 3 times than that in AnBF (p < 0.05). Owing to their powerful ability to destroy benzene, Rhodoplanes and Bradyrhizobium are capable of metabolizing sulfonamides (Chen et al., 2022; Wang et al., 2022). It is worth mentioning that SMX was the sole sulfur source flowing into two BFs. As the typical sulfur-reducing bacteria, a high abundance of Desulfomonile in BioCF meant a high transformation capacity for SMX. For AnBF, Geobacter and Nitrospira were significantly enriched (p < 0.05), of which the relative abundance increased by over 7 times more than that in BioCF. Geobacter was reported to be susceptible and protect themselves from being killed

by secreting more proteins and accelerating biofilm formation when exposed to antibiotics (Zhou et al., 2017). As for *Nitrospira*, it is resistant to many antibiotics and the dominant host of eARGs and iARGs in activated sludges (Wang et al., 2021). These results indicated that microbial communities with different metabolic functional potentials were enriched in two BFs. Microbes in AnBF may choose to secrete a lot of EPS or activate ARGs, while microbes in BioCF can degrade SMX when facing SMX exposure. These functional responses in biofilms played a crucial role in the accumulation of ARG and in shaping microbial resistomes. In the following section, the response mechanisms toward SMX stresses concerning related metabolic pathways were elucidated using metagenomic and proteomic analysis.

3.4. Response mechanisms of microbial metabolism

3.4.1. SOS response

Antibiotic stress has the capacity to disturb microbial physiological metabolism and induce microorganisms to produce excess reactive oxygen species (ROS), which may damage DNA and activate SOS response (Andersson and Hughes, 2014). As Fig. 4b showed, the abundance of genes rec family (RecA and RecX), which regulates the DNA damageinducible protein, and lexA involved in the SOS response in AnBF was significantly 2.1–3.9 times higher than that in BioCF (p < 0.05). This further proved the above deduction that microbes suffered from much less SMX stress under the sheltering effects of biochar pores. As reported by previous literature, the triggered SOS response would promote the activation and horizontal gene transfer (HGT) of antibiotic resistance because of the stimulations on conjugation-related genes and conjugational recombination. It was consistent with the results of MGEs (Fig. 3b). This also explained why the lower abundance of sul-ARGs and resistomes accumulated in microbial biofilms in BioCF (Fig. 2 and Fig. 3).

As a vital mechanism of antibiotic resistance, antibiotic efflux pumps played a crucial protective role against exogenous antibiotic stress. In this study, SMX exposure activated the multi-drug efflux pump system, including resistance-nodulation-cell division antibiotic efflux (RND), ATP-binding cassette antibiotic efflux (ABC), and significant facilitator

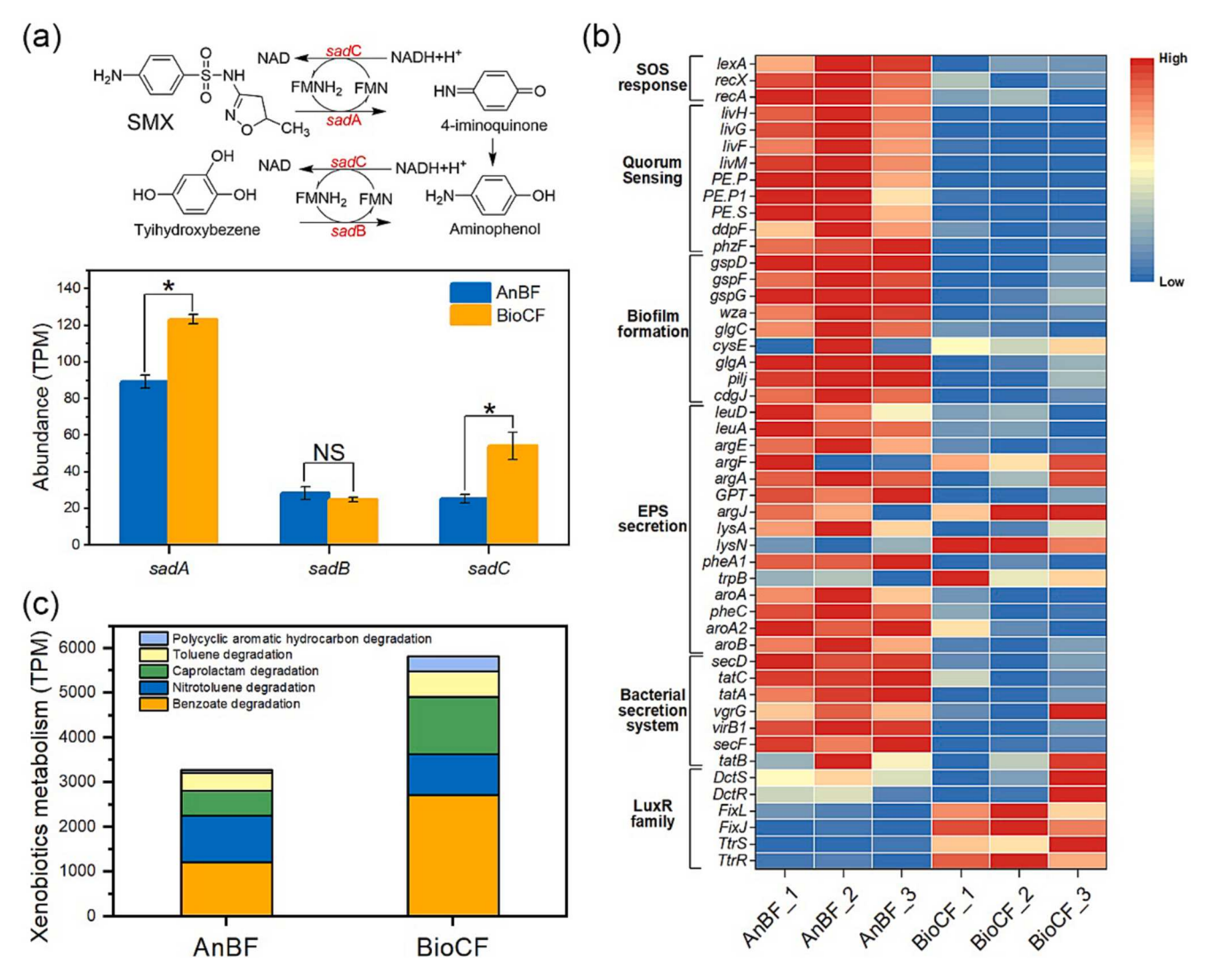


Fig. 4. Metagenomics analysis of genes associated with microbial metabolism. (a) The relative abundance of sadA, sadB and sadC related to SMX biotransformation. (b) Metagenomic analysis of genes related to quorum sensing, biofilm formation, EPS secretion bacterial secretion system and LuxR family. (c) The relative abundance of genes related to xenobiotics biodegradation and metabolism in the biofilm samples.

superfamily antibiotic efflux (MFS) (see Supplementary materials). The abundance of functional genes related to antibiotic efflux, such as qacL, adeF, and mefB, in AnBF, was 3.1–11.2 fold higher than in BioCF (p < 0.05). These findings indicated that a multidrug efflux-pump system was promoted in AnBF, thus enhancing the microbial transportation of SMX across the lipid bilayer from intracellular matrices to extracellular matrices. Metaproteomic analysis showed the significant upregulation of ABC transporters related to the antibiotic efflux system in AnBF (p < 0.05) (Fig. 5). The above results suggested that higher SMX exposure to microbes in AnBF activated the SOS response and promoted the antibiotic efflux system against exogenous SMX stress.

3.4.2. EPS excretion and biofilm formation

In addition to the activation and acquisition of antibiotic resistance, EPS secretion, biofilm formation, and strengthening interspecies cooperation, they also acted as effective ways for microorganisms to withstand antibiotic-induced stress. In this study, the abundance of several functional genes (e.g., gspD, wza, glgc, gspF, argF, argA, GPT, and pheA1) that encoded enzymes involved in biofilm formation and EPS secretion dramatically increased (p < 0.05) in AnBF (Fig. 4b). This indicated that microbes in AnBF produced and secreted more EPS, especially tyrosine, tryptophan and lysine, which are the primary EPS components and played an essential role against antibiotic toxic effects by absorbing and

complexing them. Higher EPS quantitate contents also verified the hypothesis (Fig. 1f). Quorum sensing, as a microbial cell-cell chemical communication process, promotes microbial bioaggregation by regulating the EPS content and proportion. A similar trend was also observed for genes involved in quorum sensing (e.g., livH, livG, livF, PE.S, ddpF) in the AnC biofilm samples (Fig. 4b). This indicated that microbial community in AnBF may accelerate the formation of tight bio-aggregates. Analysis of biofilm morphology showed that a compact and dense biofilm colonized the AnC surface. The thicker biofilm and higher EPS contents would effectively reduce the breakthrough into the interior of biofilms and microbial uptake of exogenous antibiotics. Collectively, compared to BioCF, a higher abundance of functional genes involved in EPS secretion, biofilm formation, and quorum sensing in AnBF meant microbes may choose to build a dense biofilm and excrete more EPS to lower the exposure and uptake of SMX against exogenous antibiotic stress.

3.4.3. SMX biotransformation

Vila-Costa et al. (2017) suggested that antibiotic biodegradation and ARG dispersal are the two dominant mechanisms of microbial resistance in river water and cobble biofilms. The effect of SMX biotransformation on the cutdown of SMX selection stress should also be paid attention. Importantly, FMNH2-dependent monooxygenase (sadA), flavin

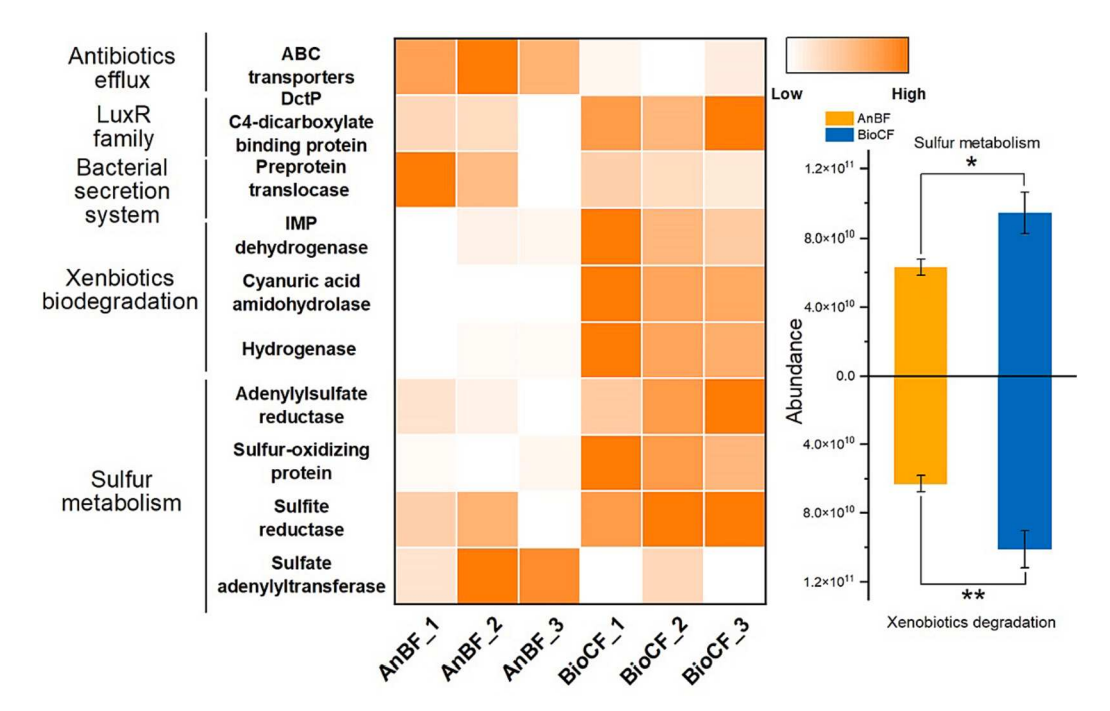


Fig. 5. Metaproteome analysis of the key proteins related to antibiotics efflux, LuxR family, bacterial secretion system, xenobiotics biodegradation, sulfur metabolism and the relative abundance. Note: *, p < 0.05; **, p < 0.01; NS, no significance.

monooxygenase (sadB), and FMN reductase (sadC) trigger the initial ipso-hydroxylation and subsequent cleavage of sulfonamides (Reis et al., 2018). The reaction pathways are shown in Fig. 4a. Metagenomic analysis indicated that the relative abundance of sadA and sadC in BioCF was 1.4–2.2 fold higher than that in AnBF (p < 0.01). The accumulated abundance of other functional genes involved in xenobiotics biodegradation and metabolism, including benzoate degradation, nitrotoluene degradation, and caprolactam degradation, in BioCF, also significantly increased by 77.3 % (p < 0.05). Metagenomic analysis showed that genes related to xenobiotics biodegradation and metabolism encoding IMP dehydrogenase, cyanuric acid amidohydrolase, and hydrogenase, which may participate in SMX degradation, were significantly upregulated (p < 0.05) (Fig. 5). It was worth mentioning that SMX was the sole sulfur source in this experiment. As Fig. 5 illustrated, the functional genes related to sulfur metabolism, such as adenylylsulfate reductase, sulfur-oxidizing protein, sulfite reductase, and sulfate adenylyltransferase in BioCF, all showed an upregulated expression. This indicated microbes in BioCF showed a more substantial capacity for the biotransformation of sulfur-containing xenobiotics. In addition, the batch tests of SMX biodegradation showed faster degradation kinetics for microbes in BioCF in comparison with AnCF as well (Fig. 1h). In summary, the above results all suggested that compared to AnBF, microbes in BioCF held a more substantial capacity for SMX biotransformation to defense against exogenous SMX stress.

Interestingly, microbes colonizing in BioCF held a higher SMX degradation capacity despite the lower SMX uptake or exposure reflected by SOS response. The LuxR family signaling system is regarded as a critical regulator that controls the synthesis and excretion of exoenzymes (Li et al., 2022; Zhong et al., 2021). Compared with AnBF, the relative abundance of functional genes in LuxR family (e.g., *DctS*, *DctR*, *FixL*, *TtrS*, and *TtrR*) in BioCF were significantly higher (p < 0.05) (Fig. 4). DctP, a C4-dicarboxylate binding protein of the LuxR family, was detected to be upregulated in BioCF (Fig. 5). These implied that microbes may achieve SMX biotransformation by the excretion of extracellular degradation enzymes. The molecular weights of these functional enzymes were 11.264–71.565 kDa, and the corresponding molecular sizes were between 2 and 8 nm (Lu et al., 2022); thus, they could enter the mesopores of biochar. Regarding the similar abundance

of genes and proteins related to the bacterial secretion system between AnBF and BioCF, it can be inferred that most of the functional units of the bacterial secretion system for AnBF were applied for the antibiotics efflux and EPS excretion. In contrast, the excretion of extracellular enzymes in BioCF dominated their use.

3.5. Roles of biochar pores in alleviating ARG accumulation

In the last decade, researchers worldwide have promoted the application of biochars to reduce the transport of manure-derived antibiotics into natural environments, such as the construction of decentralized biofiltration systems and wetlands using biochars. Owing to the high affinity for antibiotics and microbes of biochar, biofilms in the biocharbased biofiltration systems would evolve into ideal reservoirs for the development and spread of ARGs, where severe environmental risks existed. The properties of biochars, especially pore distribution, have been proven to affect the microbial community and metabolism of biofilms colonizing on it (Lu et al., 2022), potentially influencing the resistomes. However, the relationships between biochar properties and microbial resistomes of biofilms colonizing on it are still unclear. Studying this can help the selection and optimization of filter media to mitigate the accumulation and spread of ARGs in biofiltration systems. Here, the effects of biochar pores on ARG accumulation in biofiltration systems under long-term SMX exposure were evaluated using the qPCR approach, and the microbial response mechanism was elucidated using metagenomic and metaproteomic analysis.

Surprisingly, the experimental groups (BioCF) and control groups (AnBF) all maintained high TOC performance, indicating that microbes adapted to the conditions induced by SMX stress and maintained the system's stability. Zhao et al., 2021 reported that lab-scale anaerobic sequence batch reactors still held a stable COD removal efficiency (>90 %) under high sulfonamide stress (5 mg/L) through the EPS secretion, biofilm formation, and ARGs activation. And much higher EPS contents and denser biofilm can explain why AnBF held a slightly better TOC performance. Interestingly, a much lower abundance of sul-ARGs resistomes and MGEs accumulated in BioCF, though the SMX removal of BioCF was about 3-fold higher than AnBF. Combined with the adsorption kinetics and quantitative analysis of sorbed SMX, it was

found that the sheltering effects of biochar pores played a vital role in relieving the stress of retained SMX and mitigating the ARG accumulation. Much sorbed SMX were restricted in micropores and macropores of biochars and then became un-bioavailable due to steric hindrances (Wang et al., 2020). This also reduced the environmental risks of secondary pollution of the biofiltration systems in terms of the sorbed but incompletely mineralized antibiotics (Liu et al., 2019). Meanwhile, based on the results of the microbial community analysis, the microbial community and dominant genera between BioCF and AnBF were significantly different. Potential SMX degraders, Rhodoplanes, Bradyrhizobium, and Desulfomonile, were enriched in BioCF while typical SMX-tolerant microbial genera, Geobacter and Nitrospira, became dominant in AnBF under long-term SMX exposure. Biochar filters were reported to promote the colonization of heterotrophic bacteria able to degrade different kinds of organic matter, i.e., genus Sphingomonas and Gemmata (Liu et al., 2017; Guo et al., 2022). Thus, it can be concluded that microbes in BioCF and AnBF adopted distinct response strategies to cope with SMX stress, as illustrated in Fig. 6.

For microbes in AnBF, much sorbed SMX by AnC were assimilated and entered in microbial cells. Subsequently, the microbial multiple response systems were activated. For example, the antibiotic resistancemediated SOS response was activated to relieve the cell damage induced by SMX. Multi-drug efflux genes (ABC-type, RND-type, and MFS-type efflux) were upregulated to pump intracellular SMX out via the efflux pump system. The discharged SMX can still be taken in by other adjoin microbes and activate ARGs. Moreover, the upregulation of functional genes related to quorum sensing, EPS secretion, and biofilm formation (i.e., gspD, wza, livH, livG) accelerated the formation of dense biofilm. It can act as an effective barrier to block the entrance of sorbed SMX by tightly binding with the antibiotics. However, SMX retained in biofilms were likely to be assimilated by the adjoin microbes and suppressed the growth and metabolism of hosts (Jia et al., 2022). A few intracellular SMXs would also be degraded into less toxic organic compounds by sadABC enzymes and other non-specific enzymes (e.g., dehydrogenase and sulfite reductase). For microbes in BioCF, in comparison to AnBF, the downregulation of RexA, RexC, and lexA genes meant biochar pores reduced the SMX uptake and lowered SOS response in BioCF, as well as the antibiotics efflux. In BioCF, quorum sensing and biofilm formation genes were also downregulated. Instead, functional genes related to SMX transformation (sadABC, xenobiotics degradation and metabolism, and sulfur metabolism) were upregulated. These implied that microbes in BioCF were selected to degrade the intracellular and extracellular SMX other than EPS secretion or biofilm formation for defense against SMX exposure. This was helpful in relieving the stress of retaining SMX effectively and reducing its environmental risks. The associations among pores distributions, bioavailability regulation of sorbed antibiotics, and affected microbial community and metabolism required further exploration and elucidation. Collectively, these findings demonstrated that biochar pores can effectively mitigate ARG accumulation in biofiltration systems via the stress relieving of retained SMX and change of microbial defense strategy. The above results can supply insight into the microbial response mechanisms to SMX. They thus can provide a basis for the selection and optimization of biochar to mitigate the ARGs accumulation and dissemination in biofiltration systems when dealing with antibiotic-contaminated pollution.

4. Conclusion

Our study investigated the effect of biochar pores on ARG accumulation in biofiltration systems and microbial metabolism response to SMX stress. Results showed that biochar pores effectively reduced sul-ARG accumulation, as well as the resistomes and MGEs. Functional genera potentially involved in SMX biotransformation were enriched. Metagenomic and metaproteomic analysis demonstrated that biochar pores induced the changeover of microbial defense strategy against SMX from blocking SMX uptake by EPS absorbing to SMX biotransformation.

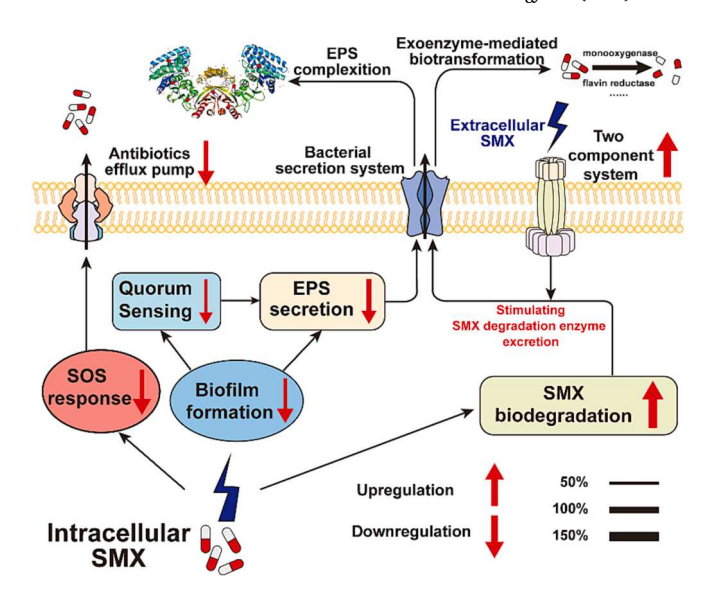


Fig. 6. Proposed model for the microbial metabolism response towards the SMX stress under the effects of biochar pores. The arrow width indicated the response degrees of the related metabolism pathways in BioCF in comparison to AnBF.

This study can provide a basis for the selection and optimization of biochar to mitigate ARG accumulation and dissemination in biofiltration systems when facing antibiotic pollution.

CRediT authorship contribution statement

Lecheng Wei: Conceptualization, Data curation, Formal analysis, Investigation, Methodology, Software, Writing – original draft, Writing – review & editing. Jingjing Zheng: Conceptualization, Data curation, Methodology, Writing – original draft. Yutong Han: Formal analysis, Software, Writing – review & editing. Xiangyang Xu: Conceptualization, Methodology, Writing – review & editing. Mengyan Li: Conceptualization, Funding acquisition, Writing – review & editing. Liang Zhu:

Declaration of competing interest

The authors declare that they have no known competing financial interests or personal relationships that could have appeared to influence the work reported in this paper.

Data availability

Data will be made available on request.

Acknowledgement

This work was financially supported by the National Natural Science Foundation of China (51961125101). Li was supported by the National Science Foundation (CBET-1903597) and the US Department of Agriculture (NIFA 2019-67020-30475).

Appendix A. Supplementary data

Supplementary data to this article can be found online at https://doi.org/10.1016/j.biortech.2023.130257.

References

- Ajibade, F.O., Yin, W., Guadie, A., 2023. Impact of biochar amendment on antibiotic removal and ARGs accumulation in constructed wetlands for low C/N wastewater treatment. Chem. Eng. J. 459, 141541.
- Andersson, D.I., Hughes, D., 2014. Microbiological effects of sublethal levels of antibiotics. Nat. Rev. Microbiol. 12 (7), 465–478.
- Chen, C., Fang, Y., Zhou, D., 2023. Selective pressure of PFOA on microbial community: enrichment of denitrifiers harboring ARGs and the transfer of ferric-electrons. Water Res. 233, 119813.
- Chen, J., Yang, Y., Ke, Y., 2022. Sulfonamide-metabolizing microorganisms and mechanisms in antibiotic-contaminated wetland sediments revealed by stable isotope probing and metagenomics. Environ. Int. 165, 107332.
- Deng, S., Chen, J., Chang, J., 2021. Application of biochar as an innovative substrate in constructed wetlands/biofilters for wastewater treatment: performance and ecological benefits. J. Clean Prod. 293, 126156.
- Guo, J., Li, J., Chen, H., 2017. Metagenomic analysis reveals wastewater treatment plants as hotspots of antibiotic resistance genes and mobile genetic elements. Water Res. 123, 468–478.
- Guo, F., Xu, F., Cai, R., Li, D., Xu, Q., Yang, X., Wu, Z., Wang, Y., He, Q., Ao, L., Vymazal, J., Chen, Y., 2022. Enhancement of denitrification in biofilters by immobilized biochar under low-temperature stress. Bioresour. Technol. 347, 126664.
- Guo, X., Yang, Y., Lu, D., 2018. Biofilms as a sink for antibiotic resistance genes (ARGs) in the Yangtze estuary. Water Res. 129, 277–286.
- Jia, Y., Wang, P., Ou, Y., Yan, Y., Zhou, S., Sun, L., Lu, H., 2022. Insights into the microbial response mechanisms to ciprofloxacin during sulfur-mediated biological wastewater treatment using a metagenomics approach. Water Res. 223, 118995.
- Li, Z., Li, X., Xia, H., 2022. Roles of LuxR-family regulators in the biosynthesis of secondary metabolites in actinobacteria. World J. Microbiol. Biotechnol. 38 (12), 250.
- Liang, J., Lin, H., Singh, B., 2023. A global perspective on compositions, risks, and ecological genesis of antibiotic resistance genes in biofilters of drinking water treatment plants. Water Res. 233, 119822.
- Liu, C., Chuang, Y., Li, H., Boyd, S.A., Teppen, B.J., Gonzalez, J.M., Johnston, C.T., Lehmann, J., Zhang, W., 2019. Long-term sorption of lincomycin to biochars: The intertwined roles of pore diffusion and dissolved organic carbon. Water Res. 161, 108–118
- Liu, F., Zhang, S., Luo, P., 2018. Purification and reuse of non-point source wastewater via myriophyllum-based integrative biotechnology: A review. Bioresour. Technol. 248, 3–11.
- Liu, H., Zhu, L., Tian, X., Yin, Y., 2017. Seasonal variation of bacterial community in biological aerated filter for ammonia removal in drinking water treatment. Water Res. 123, 668–677.
- Lu, Z., Sun, W., Li, C., 2020. Effect of granular activated carbon pore-size distribution on biological activated carbon filter performance. Water Res. 177, 115768.
- Lu, Z., Jing, Z., Huang, J., 2022. Can we shape microbial communities to enhance biological activated carbon filter performance? Water Res. 212, 118104.

- Oberoi, A.S., Jia, Y., Zhang, H., 2019. Insights into the fate and removal of antibiotics in engineered biological treatment systems: a critical review. Environ. Sci. Technol. 53 (13), 7234–7264.
- Reis, A.C., Čvančarová, M., Liu, Y., Lenz, M., Hettich, T., Kolvenbach, B.A., Corvini, P.F. X., Nunes, O.C., 2018. Biodegradation of sulfamethoxazole by a bacterial consortium of Achromobacter denitrificans PR1 and leucobacter sp. GP. Appl. Microbiol. Biotechnol. 102 (23), 10299–10314.
- Su, J., Wei, B., Ou-Yang, W., 2015. Antibiotic resistome and its association with bacterial communities during sewage sludge composting. Environ. Sci. Technol. 49 (12), 7356–7363.
- Tang, T., Chen, Y., Du, Y., 2023. Effects of functional modules and bacterial clusters response on transmission performance of antibiotic resistance genes under antibiotic stress during anaerobic digestion of livestock wastewater. J. Hazard. Mater. 441, 129870.
- Vignola, M., Werner, D., Hammes, F., 2018. Flow-cytometric quantification of microbial cells on sand from water biofilters. Water Res. 143, 66–76.
- Vila-Costa, M., Gioia, R., Aceña, J., 2017. Degradation of sulfonamides as a microbial resistance mechanism. Water Res. 115, 309–317.
- Wang, J., Man, Y., Ruan, W., 2022. The effect of rhizosphere and the plant species on the degradation of sulfonamides in model constructed wetlands treating synthetic domestic wastewater. Chemosphere 288, 132487.
- Wang, B., Zhang, Y., Zhu, D., 2020. Assessment of bioavailability of biochar-sorbed tetracycline to Escherichia coli for activation of antibiotic resistance genes. Environ. Sci. Technol. 54 (20), 12920–12928.
- Wang, Y., Zhao, R., Liu, L., 2021. Selective enrichment of comammox from activated sludge using antibiotics. Water Res. 197, 117087
- Xu, L., Campos, L.C., Canales, M., 2020. Drinking water biofiltration: Behaviour of antibiotic resistance genes and the association with bacterial community. Water Res. 182, 115954.
- Zhang, H., Jia, Y., Khanal, S.K., 2018. Understanding the role of extracellular polymeric substances on ciprofloxacin adsorption in aerobic sludge, anaerobic sludge, and sulfate-reducing bacteria sludge systems. Environ. Sci. Technol. 52 (11), 6476–6486.
- Zhao, Q., Guo, W., Luo, H., 2021. Deciphering the transfers of antibiotic resistance genes under antibiotic exposure conditions: Driven by functional modules and bacterial community. Water Res. 205, 117672.
- Zheng, J., Chen, T., Chen, H., 2018. Antibiotic resistome promotion in drinking water during biological activated carbon treatment: Is it influenced by quorum sensing? Sci. Total Environ. 612. 1–8.
- Zhong, X., Lu, R., Liu, F., 2021. Identification of LuxR family regulators that integrate into quorum sensing circuit in Vibrio parahaemolyticus. Front Microbiol 12.
- Zhou, L., Li, T., An, J., 2017. Subminimal inhibitory concentration (sub-MIC) of antibiotic induces electroactive biofilm formation in bioelectrochemical systems. Water Res. 125, 280–287.
- Zhu, X., Chen, B., Zhu, L., 2017. Effects and mechanisms of biochar-microbe interactions in soil improvement and pollution remediation: a review. Environ. Pollut. 227,
- Zhu, Y.G., Zhao, Y., Li, B., 2017. Continental-scale pollution of estuaries with antibiotic resistance genes. Nat. Microbiol. 2.